Citation: Molecular Therapy—Nucleic Acids (2016) 5, e359; doi:10.1038/mtna.2016.63
Official journal of the American Society of Gene & Cell Therapy
www.nature.com/mtna

Effects of Fibrotic Tissue on Liver-targeted Hydrodynamic Gene Delivery

Yuji Kobayashi[1], Kenya Kamimura[1], Hiroyuki Abe[1], Takeshi Yokoo[1], Kohei Ogawa[1], Yoko Shinagawa-Kobayashi[1], Ryo Goto[1], Ryosuke Inoue[1], Masato Ohtsuka[2,3], Hiromi Miura[4], Tsutomu Kanefuji[1], Takeshi Suda[1], Masanori Tsuchida[5], Yutaka Aoyagi[1], Guisheng Zhang[6], Dexi Liu[6] and Shuji Terai[1]

Hydrodynamic gene delivery is a common method for gene transfer to the liver of small animals, and its clinical applicability in large animals has been demonstrated. Previous studies focused on functional analyses of therapeutic genes in animals with normal livers and little, however, is known regarding its effectiveness and safety in animals with liver fibrosis. Therefore, this study aimed to examine the effects of liver fibrosis on hydrodynamic gene delivery efficiency using a rat liver fibrosis model. We demonstrated for the first time, using pCMV-Luc plasmid, that this procedure is safe and that the amount of fibrotic tissue in the liver decreases gene delivery efficiency, resulting in decrease in luciferase activity depending on the volume of fibrotic tissue in the liver and the number of hepatocytes that are immunohistochemically stained positive for transgene product. We further demonstrate that antifibrotic gene therapy with *matrix metalloproteinase-13* gene reduces liver fibrosis and improves efficiency of hydrodynamic gene delivery. These results demonstrate the negative effects of fibrotic tissue on hydrodynamic gene delivery and its recovery by appropriate antifibrotic therapy.

Molecular Therapy—Nucleic Acids (2016) **5**, e359; doi:10.1038/mtna.2016.63; published online 30 August 2016
Subject Category: Mechanisms of gene and nucleic acid transfer/transfection

Introduction

Despite the progress achieved in developing therapeutic options for viral hepatitis, such as treatment with antiviral agents, no standard therapy has been developed for liver fibrosis. Liver fibrosis (LF) is considered the final stage of all chronic liver diseases induced not only by chronic viral hepatitis but also by autoimmune hepatitis, nonalcoholic steatohepatitis, congenital fibrosis, and alcoholic liver injury. Millions of people are affected by the symptoms and complications of LF, such as hepatic failure, jaundice, encephalopathy, liver cancer, and gastrointestinal bleeding.[1,2] Antifibrotic gene therapy has been studied and shown to be effective in controling fibrogenesis[3] by targeting the production and deposition of extracellular matrix activated hepatic stellate cells.[1,2] In these studies, various gene delivery systems were examined, including viral vectors,[4–9] chemical carriers,[9–11] and physical methods.[9,12,13] Because chronic viral hepatitis is the major etiology of LF,[1] and it causes liver cancer,[2] the viral vector and chemical methods of gene delivery are not ideal for use in LF cases, from the stand point of biological safety regarding immunogenicity and carcinogenic properties induced by the carriers. Therefore, we have focused on hydrodynamic gene delivery (HGD), one of the physical methods, to deliver genes with the physical force produced by the rapid injection of a large volume of fluid.[14] The major advantages of this procedure are (i) that there is no need for carriers and (ii) that the simple injection of naked DNA plasmid can offer therapeutic gene expression. The modification of the procedure achieved site-specific, safe, and effective gene delivery in small[15] and large animals[16–24] with the help of a procedure of image-guided liver lobe-specific catheter insertion. This method achieved a therapeutic level of gene expression in animals with no immunoreaction, or migration of plasmid DNA into other organs.[23,24]

While these previous studies focused on the applicability of the procedure and the functional analyses of therapeutic genes in animals with normal livers, little is known regarding its effectiveness and safety in animals with liver diseases leading to end-stage LF. Yeikilis *et al.* reported the phenomenon of decrease of HGD efficiency in rats with liver cirrhosis examining the mechanism of the procedure,[25] however the degree of LF on the efficiency, safety of the procedure, and the impact of antifibrotic gene therapy on its reverse have not been analyzed. The effects of fibrotic tissue on HGD are determined by the difference of gene expression between animal species, due to natural presence of fibrotic structure in the liver. For example, pigs, which are known to contain a specific amount of fibrotic liver tissue to support their bodies, show 100- to 1,000-fold lower gene delivery efficiency than dogs and baboons[3,22–24] (Kamimura K., unpublished data), when the same gene delivery procedure was used. Although

The first two authors contributed equally to this work..
[1]Division of Gastroenterology and Hepatology, Graduate School of Medical and Dental Sciences, Niigata University, Niigata, Niigata, Japan; [2]Department of Molecular Life Science, Division of Basic Medical Science and Molecular Medicine, School of Medicine, Tokai University, Isehara, Kanagawa, Japan; [3]The Institute of Medical Sciences, Tokai University, Isehara, Kanagawa Japan; [4]Department of Regenerative Medicine, Basic Medical Science, School of Medicine, Tokai University, Isehara, Kanagawa, Japan; [5]Division of Thoracic and Cardiovascular Surgery, Graduate School of Medical and Dental Sciences, Niigata University, Niigata, Niigata, Japan; [6]Department of Pharmaceutical and Biomedical Sciences, College of Pharmacy, University of Georgia, Athens, Georgia, USA. Correspondence: Kenya Kamimura, Division of Gastroenterology and Hepatology,Graduate School of Medical and Dental Sciences, Niigata University, 1–757 Asahimachi–dori, Chuo–ku, Niigata, Niigata, 9518510, Japan. E-mail: kenya-k@med.niigata-u.ac.jp
Keywords: gene therapy; hydrodynamic gene delivery; liver fibrosis; MMP13; nonviral gene delivery
Received 7 July 2016; accepted 7 July 2016; advance online publication 30 August 2016. doi:10.1038/mtna.2016.63

these phenomena were observed at the experimental level, it becomes important to understand the effects of fibrotic tissue on gene delivery not only for treatment of advanced LF but also for treatment of liver diseases that eventually lead to end-stage fibrosis.

For this purpose, in this study, we have systematically examined the effect of fibrotic tissue on efficiency of HGD using a rat model of LF. In addition, we have tested whether antifibrotic gene therapy can improve the gene delivery efficiency in this model using HGD of *matrix metalloproteinase 13* (*MMP13*) gene.[12] Our results showed, for the first time, that the amount of fibrotic tissue in cirrhotic livers decreases gene expression in the liver depending on the volume of fibrotic tissue and that *MMP13* gene therapy preserves efficiency of HGD in fibrotic livers.

Results

Effects of fibrosis on the efficiency of liver-targeted HGD

The LF animal model was developed by bile duct ligation (BDL) in rats according to the previously published procedure.[8,10,12,26–29] Sirius red staining was used to assess the distribution of the fibrotic tissue, and the fibrotic level in the entire liver was assessed 9 weeks after the procedure (**Figure 1**). Quantitative analysis showed 10.95±2.43% of fibrotic tissue in the LF group, which was statistically higher than normal control (2.77±0.87%, $P < 0.01$, **Figure 1a**). The level of the LF in each lobe was analyzed to determine the fibrotic tissue distribution. The right lateral, right medial, left medial, left lateral, and caudate lobes in LF rats showed homogeneous 8.11, 8.65, 13.4, 12.9, and 11.7% of fibrotic tissue, respectively, whereas in normal rats, they showed 3.50, 3.36, 3.06, 2.56, and 1.35% (N.S.), respectively. This homogeneous distribution of the fibrotic tissue and the statistical difference between LF and normal rats suggest the efficiency of BDL for developing homogeneous LF in the LF group (**Figure 1b**).

To examine the effects of fibrotic tissue on the efficiency of the HGD, pCMV-Luc DNA solution, with a concentration of 5 μg/ml and a volume of 5% body weight, was hydrodynamically delivered into normal rats and LF rats 9 weeks after BDL using the liver-targeted HGD procedure. Animals

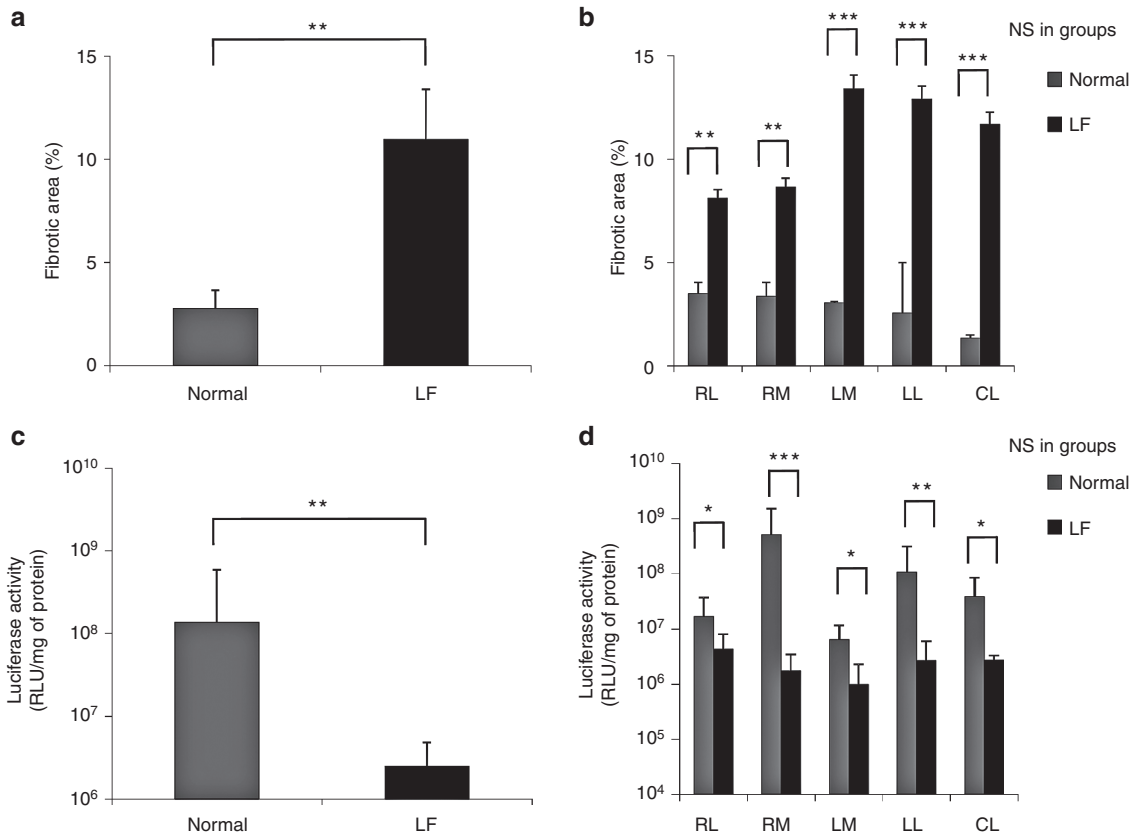

Figure 1 Effect of fibrosis on the efficiency of hydrodynamic gene delivery. (**a**) The standard Sirius red staining was performed to evaluate the fibrotic liver tissues in normal rats and LF rats 9 weeks after bile duct ligation. A quantitative analysis of fibrotic tissue positively stained was performed using ImageJ software (version 1.6.0_20, National Institutes of Health) as previously reported (a total of 75 sections from three rats each were analyzed). (**b**) The distribution of the fibrotic area (%) in each lobe (15 sections from all lobes). The values represent mean ± SD. (**c**) Each group of three normal rats and LF rats were hydrodynamically injected with pCMV-Luc, and liver samples were collected 4 hours after the transfection followed by the standard luciferase assay. The values represent mean ± SD (five samples from every liver lobe per rat from all three rats in each group, yielding 15 samples per group). (**d**) Luciferase activity in each lobe of the rat groups (three tissue samples from each lobe). *$P < 0.05$,** $P < 0.01$, *** $P < 0.001$, and N.S., no statistical significance. *t*-test or one-way analysis of variance (ANOVA) followed by Bonferroni's multiple comparison test. LF, liver fibrosis group; RL, right lateral lobe; RM, right medial lobe; LM, left medial lobe; LL, left lateral lobe; and CL, caudate lobe.

were euthanized 4 hours after gene delivery of pCMV-Luc plasmid, and the liver tissue was collected. The level of luciferase activity was assessed using the standard luciferase assay (**Figure 1c**,**d**). The luciferase activity showed a luciferase level of 2.5×10^6 relative light units (RLU)/mg of protein in the LF group, which was statistically lower than 1.4×10^8 obtained in normal rats ($P < 0.01$) (**Figure 1c**). Each liver lobe in the LF group showed no significant difference, indicating the homogeneously lower level of luciferase activity in fibrotic liver owing to the homogeneous fibrotic tissue (**Figure 1b**,**d**). These results suggest the successful development of homogeneous LF in rats, and that fibrotic tissue significantly reduced the gene delivery efficiency of the liver-targeted HGD.

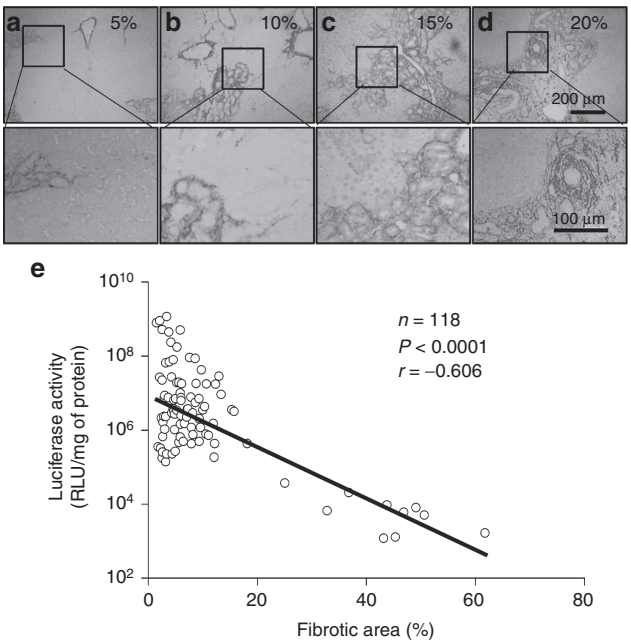

Figure 2 Correlation between liver fibrosis and efficiency of liver-targeted HGD (**a–d**) representative images of Sirius red staining; (**a**) ~5% of fibrotic tissue, (**b**) for 10%, (**c**) for 15%, and (**d**) for 20%. (**e**) Correlation analysis between area of fibrotic liver tissue and luciferase activity ($n = 120$, *** for $P < 0.001$); Scale bar represents 200 µm (100 ×). *r*, correlation coefficient.

Correlation between LF and gene delivery efficiency

To determine the relationship between LF and gene delivery efficiency, the amount of fibrotic liver tissue and gene delivery efficiency was analyzed (**Figure 2**) using Sirius red staining and luciferase gene expression. Representative Sirius red staining images show ~5, 10, 15, and 20% of fibrotic tissue in the liver (**Figure 2a–d**). The linear regression between the area of LF and luciferase activity is shown in **Figure 2e** and a significant negative correlation was evidenced ($r = -0.606$, $P < 0.001$). These results suggest that the fibrotic liver tissue directly decreased the efficiency of the liver-targeted HGD.

Safety of liver-targeted HGD to fibrotic liver

The safety of the procedure was assessed with the careful confirmation of the physiological condition of the animals using serum biochemical analyses (see **Supplementary Figure S1**). No significant damage to the internal organs was seen in LF rats, and no difference was seen in the recovery from anesthesia. The biochemical analyses performed at appropriate time points after HGD on LF rats 10 weeks after BDL showed a transient increase in hepatic enzymes: aspartate aminotransferase, 435.1 ± 322.4 IU/l; alanine aminotransferase, 305.1 ± 359.2 IU/l; and lactate dehydrogenase 2784 ± 1691 IU/l. This hepatic enzyme increase occurred just after the HGD (see **Supplementary Figure S1a**), which showed no significant difference compared with that in normal rats of the same size: aspartate aminotransferase, 379.5 ± 177.4 IU/l; alanine aminotransferase, 209.1 ± 52.3 IU/l; and lactate dehydrogenase, 2001 ± 584.8 IU/l (see **Supplementary Figure S1b**). The levels of these enzymes decreased in 7 days both in LF and normal rats

a

Group	BDL	HGD (MMP13)
LF	+	–
LF-MMP13	+	+

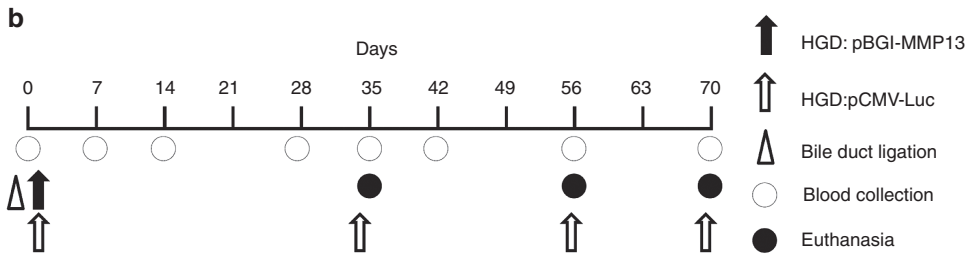

Figure 3 Experimental protocol for antifibrotic treatment. The rat liver fibrosis (LF) model was developed by the bile duct ligation (BDL) ($n = 40$). Two groups of LF ($n = 20$) and LF-MMP13, BDL simultaneously followed by hydrodynamic delivery of pBGI-MMP13 ($n = 20$) were developed. Each model was analyzed for the severity of the LF at appropriate time points using a serum marker of hyaluronic acid, type 4 collagen, albumin, and hepatobiliary enzymes. The liver-targeted hydrodynamic gene delivery (HGD) of pCMV-Luc was performed on 5 rats in each group at the time points of 0 ($n = 10$), 5 ($n = 10$), 8 ($n = 10$), and 10 ($n = 10$) weeks after BDL followed by euthanasia and the collection of tissue samples.

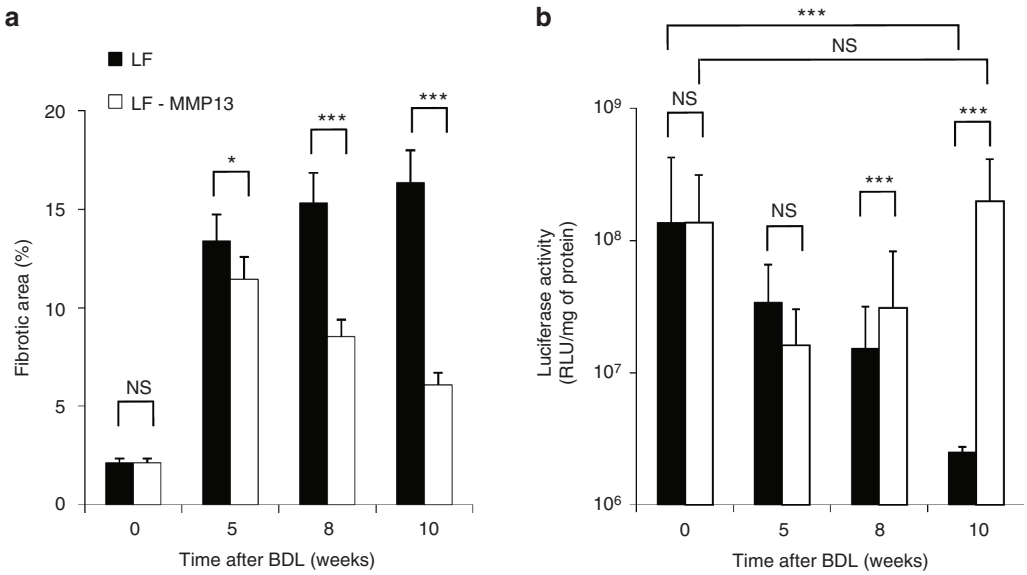

Figure 4 Effect of antifibrotic gene therapy on gene delivery efficiency. (**a**) Time-dependent change in fibrotic liver tissue. The Sirius red staining was followed by the quantitative analysis of fibrotic tissue using ImageJ software (version 1.6.0_20, National Institutes of Health). The values represent mean ± SD (five sections from five lobes of five rats each in the group, yielding 125 sections for each value from 40 rats). (**b**) Effect of the degree of liver fibrosis (LF) on hydrodynamic gene delivery. The pCMV-Luc plasmid was hydrodynamically delivered to the rats at different time post bile duct ligation (BDL) and luciferase activity in the liver was analyzed 4 hours after gene delivery. The values represent mean ± SD. (All five lobes from five rats in each group, $n = 25$ samples for each value from 40 rats) *for $P < 0.05$, ** $P < 0.01$, *** $P < 0.001$, and N.S., no statistical significance between the level in LF and LF-MMP13 groups. One-way analysis of variance (ANOVA) followed by Bonferroni's multiple comparison test.

(see **Supplementary Figure S1**). These results suggest that the liver-targeted HGD can be safely performed in LF rats, and that the decrease in gene expression is not directly caused by damage to the hepatocytes.

Effect of antifibrotic gene therapy on gene delivery efficiency

To determine whether the antifibrotic therapy for fibrotic liver can maintain/reverse the gene delivery efficiency, we examined the effect of *MMP13* therapy, which was previously reported to be effective for treating LF.[5,11,12] We have utilized the *MMP13* expressing plasmid which sustained serum MMP13 concentration for ~70 days at the highest level and showed antifibrotic effect.[12] The experimental protocol is shown in **Figure 3**. The rats were divided into two groups: rats treated with BDL (LF) and rats treated with the *MMP13* gene following BDL (LF-MMP13) (**Figure 3a**). Firstly, the BDL was performed to both groups and the liver-specific hydrodynamic delivery of the pBGI-MMP13 solution was performed on LF-MMP13 group. And they were carefully monitored for the progression of LF by histological analyses and serum marker by the collected liver and blood samples. Then, to examine the gene delivery efficiency in the fibrotic liver, the pCMV-Luc plasmid was hydrodynamically injected at appropriate time points (**Figure 3b**).

The change of fibrotic area in the livers showed a time-dependent increase in the LF group (**Figure 4a**). The liver collected 10 weeks after BDL achieved the highest level of 16.4 ± 7.67%, which was significantly higher than that of the LF-MMP13 group (6.09 ± 5.04%; $P < 0.001$). Importantly, the area of fibrotic tissue of the LF-MMP13 group showed a peak level at 5 weeks after the BDL and *MMP13* therapy, and decreased in a time-dependent manner. These results suggest that the liver-targeted *MMP13* HGD showed a time-dependent antifibrotic effect (**Figure 4a**). Then, the efficiency of the HGD was examined at selected time points (**Figure 4b**). The control rats showed the highest level of luciferase activity with the liver-targeted HGD (~1.5×10^8 RLU/mg of protein), and the activity decreased in a time-dependent manner in the LF group, with the lowest level (2.5×10^6 RLU/mg of protein) seen in animals 10 weeks after BDL. Conversely, animals in LF-MMP13 treated group showed an initial decrease in luciferase activity until 5 weeks after the procedure to the lowest level of 1.6×10^7 RLU/mg of protein. Luciferase expression level recovered from the lowest point and fully recovered in 10 weeks after the procedure with luciferase activity at 1.9×10^8 RLU/mg of protein, which was significantly higher than that of the LF group at the same time point ($P < 0.001$) (**Figure 4b**). These results suggest that the MMP antifibrotic therapy triggered the recovery of the gene delivery efficiency of the HGD by reducing the fibrotic tissue.

The number of positively stained cells with antiluciferase antibody was quantitatively analyzed in samples collected from the rats 10 weeks after BDL (**Figure 5a–d**). The level of positively stained cells indicating luciferase expression was 5.88 ± 1.37% in normal rats after HGD (**Figure 5a**). In the LF-MMP13 group, it was similar level at 6.93 ± 2.66% to none fibrotic, normal rats (N.S.) (**Figure 5c**), and significantly higher than the LF group (**Figure 5b**) with 0.92 ± 0.40% ($P < 0.05$) (**Figure 5d**).

The level of MMP13 in 10 weeks after the procedure showed similar level at 66.1 ± 10.3 pg/ml and 73.0 ± 25.6 pg/ml in normal rats and LF-MMP13 group (N.S.) and significantly higher than LF group with 9.7 ± 2.8 pg/ml (**Figure 5e**).

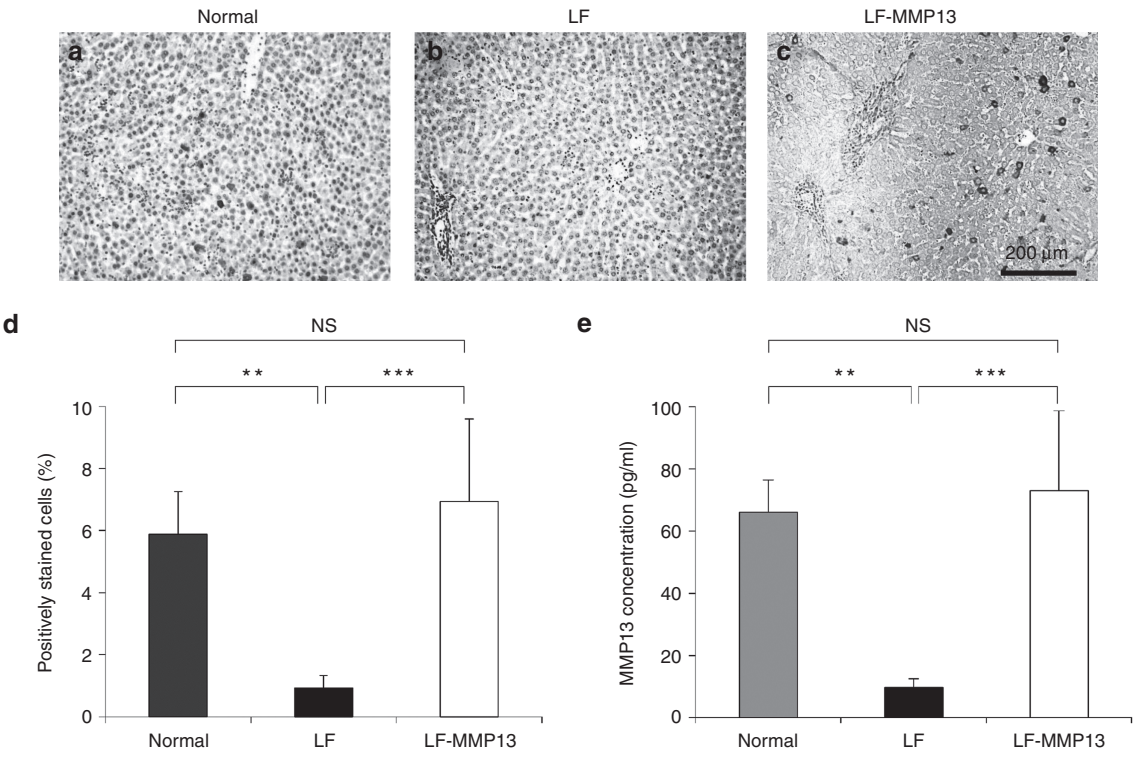

Figure 5 Histological analysis of luciferase expression in the liver. Immunohistochemical staining with antiluciferase antibody was performed on liver tissues collected 10 weeks after the treatment. Scale bar represents 200 μm (100 ×). (**a**) Normal, (**b**) liver fibrosis (LF), and (**c**) LF-MMP. (**d**) Quantitative analysis of positively stained cells. Five different liver sections from five lobes of five rats each in three groups were immunohistochemically stained with antiluciferase antibody, and a quantitative analysis was performed using ImageJ software (version 1.6.0_20, national Institutes of Health). The values represent mean ± SD. ($n = 125$ for each value) (**e**) The level of *MMP13* in 10 weeks after the procedure. Serum concentration of *MMP13* was quantified by enzyme-linked immunosorbent assay (ELISA). The values represent mean ± SD. ($n = 5$ for each group) $^{**}P < 0.01$, $^{***}P < 0.001$, and N.S., no statistical significance. One-way analysis of variance (ANOVA) followed by Bonferroni's multiple comparison test.

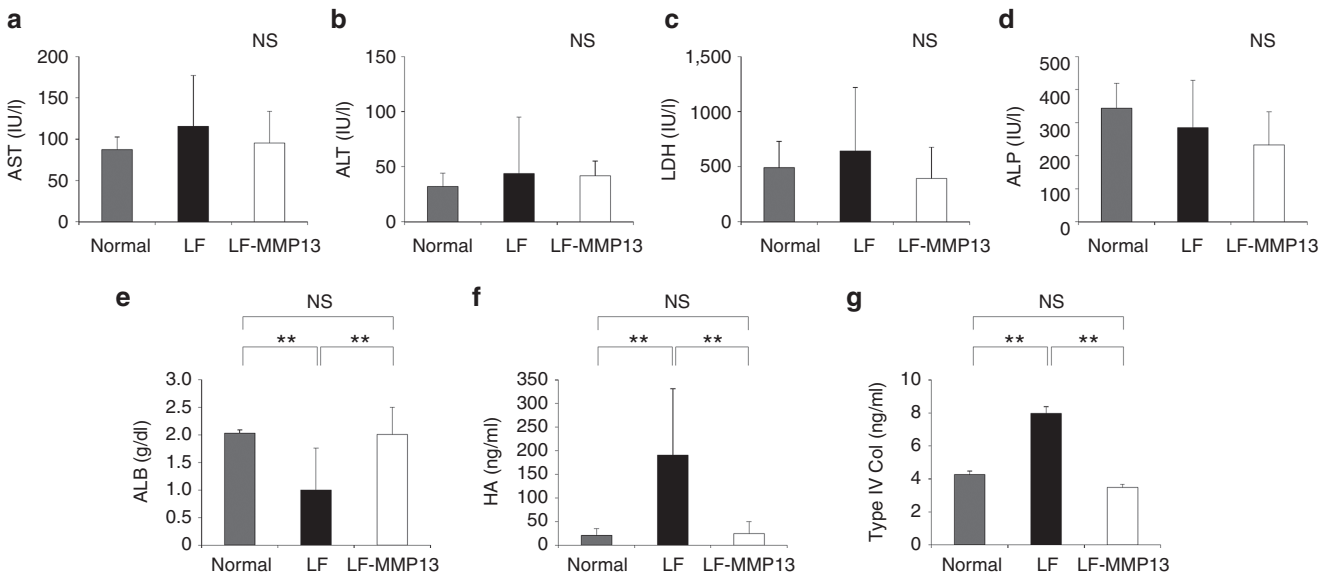

Figure 6 Serum biochemical analysis. The standard serum biochemical analysis was performed on the serum collected 10 weeks after the bile duct ligation and *MMP13* gene transfer. The values represent average concentrations of (**a**) aspartate aminotransferase (AST), (**b**) alanine aminotransferase (ALT), (**c**) lactate dehydrogenase (LDH), (**d**) alkaline phosphatase (ALP), (**e**) albumin (ALB), (**f**) hyaluronic acid (HA), and (**g**) type IV collagen (Type IV Col) in serum. The values represent mean ± SD ($n = 5$ rats for each value). * $P < 0.05$, ** $P < 0.01$, and NS, no statistical significance. One-way analysis of variance (ANOVA) followed by Bonferroni's multiple comparison test.

These results suggest that the antifibrotic therapy for the fibrotic liver decrease the level of LF, and reinstalled the capacity of liver in responding to HGD.

Biochemical analysis

To examine the recovery of the hepatic function and antifibrotic effect of the treatment, biochemical analyses were performed on blood samples collected 10 weeks after treatment (**Figure 6a–g**). No significant differences in aspartate aminotransferase (**Figure 6a**), alanine aminotransferase (**Figure 6b**), lactate dehydrogenase (**Figure 6c**), and alkaline phosphatase (**Figure 6d**) were observed (**Figure 6a–d**). However, significantly lower levels of hyaluronic acid (24.4 ± 25.0 ng/ml; **Figure 6f**) and type IV collagen (3.49 ± 1.73 ng/ml; **Figure 6g**) were observed in the LF-MMP13 group than in the LF group (190.7 ± 140.6 ng/ml; **Figure 6f**; $P < 0.05$, 7.98 ± 3.85 ng/ml; **Figure 6g**; $P < 0.01$). In addition, a statistically higher level of albumin (ALB) (2.01 ± 0.49 g/dl; **Figure 6e**) was evidenced in the LF-MMP13 group than in the LF group (1.32 ± 0.81 g/dl; **Figure 6e**; $P < 0.05$). These results suggest that the suppression of LF by *MMP13* gene transfer is the basis for the liver to regain its sensitivity to HGD by supporting the hepatic function and protein synthesis capability of the hepatocytes.

Discussion

HGD has been developed as a safe and effective method for gene transfer to the liver of small animals.[9,13,14,30] In small animals, the principle of HGD relies on a rapid tail vein injection of a volume of DNA solution equivalent to 10% of the body weight over 5 seconds.[31,32] This procedure leads to an increased pressure in the inferior vena cava and cardiac congestion that drives the solution into the hepatic veins in retrograde. The injected solution enlarges the fenestrae and induces transient hepatocyte pore formation, which allows entry of DNA solution into the hepatocytes.[31,32] Regarding efficiency of the procedure, it can achieve ~30% of hepatocytes with successful gene transfer, resulting in therapeutic effect in different animal models.[33–36] Based on this evidence, the catheter-based liver lobe-targeted HGD has been developed and was reported to achieve safe, effective, and site-specific gene delivery to the liver of large animals.[16–19,22–24,37,38] Building on these promising results, this methodology is currently under study for its further application to diseased liver, including LF, which is the final stage of various liver diseases, including viral hepatitis, alcoholic liver injury, autoimmune hepatitis, and nonalcoholic steatohepatitis, all of which may lead to liver failure and cancer at the end of pathological progression. To apply HGD to LF, we recently reported the antifibrotic effect of MMP13 using liver-targeted HGD.[12] Our results showed that the overexpression of *MMP13* in hepatocytes has a significant effect in prevention against LF, suggesting the clinical applicability of this procedure for antifibrotic liver therapy. The effect of fibrotic tissue on the efficiency of HGD was suggested in our previous study, in which we performed liver-targeted HGD in pig liver. Pig liver contains a significant amount of fibrotic tissue naturally, and we observed that the fibrotic tissue decreased the HGD efficiency.[22] Based on these previous observations using the pig liver model, we conducted the current study to examine the effects of fibrotic tissue on the efficiency of liver-targeted HGD and to further extend the applicability of HGD to later stages of fibrotic liver.

Our study clearly showed that fibrotic liver tissue reduced the gene delivery efficiency of HGD in a fibrotic tissue volume-dependent manner. In addition, successful prevention of fibrotic tissue accumulation by liver-targeted HGD of the *MMP13* gene re-established the procedure's efficiency by increasing gene expression and number of cells successfully transfected. The serum biochemical analyses showed the recovery of liver function with the increase in ALB concentration. This indicated the improvement in protein synthesis capability of hepatocytes by the *MMP13* transfection, probably owing to a reduction in the fibrotic tissue. Furthermore, the hepatocyte growth factor, which was previously reported to be useful for gene therapy for liver cirrhosis[39] and is released through *MMP13* activation,[4,5,40] seems to have contributed to such recovery. These results establish a significant correlation between fibrosis volume and gene expression by HGD, and suggest that *MMP13* gene therapy contributed to the recovery of gene expression by improving delivery efficiency and possibly hepatocyte function.

This is the first report to show the effects of fibrotic tissue on HGD efficiency and the maintenance effect of *MMP13* gene therapy on the liver. We used the BDL method to develop LF in rats, as this has been considered a model of time-dependent progression of LF[41] and has been validated in various studies.[8,10,26–29] Therefore, we saw this as the ideal model to achieve the aim of our study: to compare the gene delivery efficiency in fibrotic tissue in a volume- and time-dependent manner. Additionally, this was the only animal model allowed in our animal facility considering the strict regulations of the usage of CCl4. In this study, it is clearly demonstrated that it is desirable to start the antifibrotic treatment as early as possible once the diagnosis of liver disease is made. It is also obvious that further studies will contribute to the improvement of HGD efficiency in the fibrotic liver, focusing on the adjustment of hydrodynamic parameters, including flow rate, injection pressure, injection volume, and catheter position using various types of experimental models of LF. The strategy of optimization that we have reported in various animal species and various tissues[22,23,37] using our computer-controlled HGD system[15,42] can provide the adjustment of these parameters. Finally, a combination of the methods of removing or eluting the collagen fibers, including cell therapy,[43–45] may help improve the gene delivery efficiency and therapeutic effect of HGD in advanced LF.

In summary, we report in this study the effect of fibrotic liver tissue on the efficiency of HGD to the rat liver. Further studies are required to fine-tune the HGD parameters of our computer-controlled injection system and improve the efficiency of liver-targeted HGD in patients with extensive LF.

Materials and methods

Materials. The MMP13 expressing plasmid (pBGI-MMP13) was constructed as previously described.[12] Briefly, the plasmid contains a CAG promoter-MMP13-IRES-tdTomato-polyA cassette. The pCMV-Luc plasmid, containing firefly luciferase

cDNA driven by a CMV promoter, was purified using Plasmid Mega Kit (Qiagen, Hilde, Germany). The purity of the plasmid preparation was checked on the basis of absorbency at 260 and 280 nm and 1% agarose gel electrophoresis. Luciferase assay kits were purchased from Wako Pure Chemical Industries (Chuo-ku, Osaka, Japan). Wistar rats (n = 50, female, 200–250 g) were purchased from Japan SLC (Hamamatsu, Shizuoka, Japan).

Development of LF model and analysis of fibrotic changes. All animal experiments were approved by and conducted in full compliance with the regulations of the Institutional Animal Care and Use Committee at the Niigata University, Niigata, Japan.

LF was induced using the BDL method as previously reported.[12] In brief, the common bile duct was exposed under general anesthesia and ligated. To determine the amount of fibrotic liver tissue, liver tissue samples were collected at the appropriate time points, fixed in 10% formalin upon collection, and embedded in paraffin. Sections (10 µm) were made and standard hematoxylin and eosin staining and Sirius red staining counterstained with were performed on the samples.

Images were captured from each tissue section randomly and a quantitative analysis of fibrotic area was performed using ImageJ software (version 1.6.0_20, National Institutes of Health) as previously reported.[46]

Hydrodynamic gene delivery to rat livers. Liver-targeted HGD to the rats was performed as previously described.[15] Briefly, a midline skin incision was made on the rats under general anesthesia using isoflurane and 2,2,2-tribromoethanol (concentration, 0.016 g/ml in 0.9 % saline; dose, 1.25 ml/100 g bodyweight). An injection catheter (SURFLO 22 gauge, Terumo, Shibuya-ku, Tokyo, Japan) was inserted into the inferior vena cava and its tip was placed at the junction of the inferior vena cava and hepatic veins. Saline-containing plasmid DNA (either pBGI-MMP13 or pCMV-Luc, 5 µg/ml) was hydrodynamically injected into the liver *via* the catheter with temporal blood flow occlusions at the supra and infrahepatic inferior vena cava. Injection volume and flow rate were fixed at 5% bodyweight and 1 ml/s. The abdominal median incision was sutured after the procedure.

Luciferase assay. The HGD of pCMV-Luc plasmid DNA was performed 5, 8, and 10 weeks after the *MMP13* gene delivery. Rats were euthanized 4 hours after the injection of pCMV-Luc plasmid DNA, and tissue samples were collected from each hepatic lobe. Tissue samples for luciferase assays were kept at –80 °C until use. Lysis buffer (2 ml) (0.1 mol/l Tris–HCL, 2 mmol/l ethylenediaminetetraacetate (EDTA), and 0,1% Triton X-100; pH 7.8) was added to each sample (~200 mg wet tissue), and the samples were homogenized for 30 seconds with the tissue homogenizer (ULTRA-TURRAX T25 digital, IKA, Staufen, Germany) at maximum speed. The tissue homogenates were centrifuged in a microcentrifuge for 10 minutes at 13,000× g at 4°C. The protein concentration of the supernatant was determined using a protein assay kit (BIO-RAD, Hercules, CA) based on Coomassie blue assay strategy. Supernatant (10 µl) was mixed with luciferase assay reagent (100 ul), and the luciferase activity was measured in a luminometer (Luminescencer Octa AB-2270, ATTO, Bunkyo-ku, Tokyo, Japan) for 10 seconds according to the previously established procedure.[15]

Serum biochemical analyses. Serum biochemical markers including, AST, ALT, LDH, ALP, ALB, hyaluronic acid, and type IV collagen were analyzed by BML (Shibuya-ku, Tokyo, Japan).

Immunohistochemical staining. Tissue samples for immunohistochemical staining were collected at 2, 5, 8, and 10 weeks after BDL. All five lobes from three rats in each group were collected 4 hours after HGD of pCMV-Luc plasmids and fixed in 10% formalin upon collection before embedding in paraffin. A total of five sections (10 µm) were cut for each lobe of the rat (n = 75 per group), and standard immunohistochemistry was performed using goat antiLuciferase polyclonal antibody (G7451, 1:100 dilution; Promega, Madison, WI), Vecstain Elite ABC Goat IgG kit (PK-6105; Vector Laboratories, Burlingame, CA), and DAB chromogen tablet (Muto Pure Chemicals, Bunkyo-ku, Tokyo, Japan).

Serum MMP13 concentration. Blood samples were collected at appropriate time points and serum was used to analyze the serum level of MMP13 by enzyme-linked immunosorbent assay using Human MMP13 ELISA Kit (ELH-MMP13, RayBiothech, Norcross, GA).

Statistical analyses. The data of luciferase assays, histological analyses, and biochemical analyses were statistically evaluated by analyses of variance followed by Bonferroni's multiple comparisons test and t-test.

Supplementary material

Materials and Methods.
Figure S1. Safety of hydrodynamic gene delivery to fibrotic liver.

Acknowledgments The authors thank Nomoto M and Tsuchida T in the Division of Gastroenterology and Hepatology at the Niigata University for their excellent assistance in histological analyses. The authors also thank Fujisawa N, Maeda Y, Sasaoka T, and all staff members at the Division of Laboratory Animal Resources in Niigata University. The authors declare that they have no conflict of interest. The research in the authors' laboratories has been supported in part by Grant-in-Aid for Scientific Research from the Japanese Society for the Promotion of Sciences 22890064, 23790595, and 26860354; Takara Bio Award from JSGT; and AstraZeneca R&D Grant to K.K., 24592084 to T. M., 16K19333 to Y.T., and 26293175 to T.S.

1. Tsochatzis, EA, Bosch, J and Burroughs, AK (2014). Liver cirrhosis. *Lancet* **383**: 1749–1761.
2. Nusrat, S, Khan, MS, Fazili, J and Madhoun, MF (2014). Cirrhosis and its complications: evidence based treatment. *World J Gastroenterol* **20**: 5442–5460.
3. Abe H, Kamimura K, Yokoo T, Suda T, Kobayashi Y *et al.* (2014) Gene therapy for liver fibrosis. *JSM Gastroenterol Hepatol* **2**: 1028.
4. Iimuro Yuji, Brenner David A (2008) Matrix metalloproteinase gene delivery for liver fibrosis. *Pharm Res* **25**: 249–258.

5. Endo, H, Niioka, M, Sugioka, Y, Itoh, J, Kameyama, K, Okazaki, I *et al.* (2011). Matrix metalloproteinase-13 promotes recovery from experimental liver cirrhosis in rats. *Pathobiology* **78**: 239–252.
6. Sobrevals, L, Enguita, M, Rodriguez, C, Gonzalez-Rojas, J, Alzaguren, P, Razquin, N *et al.* (2012). AAV vectors transduce hepatocytes *in vivo* as efficiently in cirrhotic as in healthy rat livers. *Gene Ther* **19**: 411–417.
7. Siller-López, F, Sandoval, A, Salgado, S, Salazar, A, Bueno, M, Garcia, J *et al.* (2004). Treatment with human metalloproteinase-8 gene delivery ameliorates experimental rat liver cirrhosis. *Gastroenterol* **126**: 1122–33; discussion 949.
8. Iimuro, Y, Nishio, T, Morimoto, T, Nitta, T, Stefanovic, B, Choi, SK *et al.* (2003). Delivery of matrix metalloproteinase-1 attenuates established liver fibrosis in the rat. *Gastroenterol* **124**: 445–458.
9. Kamimura, K, Suda, T, Zhang, G and Liu, D (2011). Advances in Gene Delivery Systems. *Pharmaceut Med* **25**: 293–306.
10. Sato, Y, Murase, K, Kato, J, Kobune, M, Sato, T, Kawano, Y *et al.* (2008). Resolution of liver cirrhosis using vitamin A-coupled liposomes to deliver siRNA against a collagen-specific chaperone. *Nat Biotechnol* **26**: 431–442.
11. Kim, EJ, Cho, HJ, Park, D, Kim, JY, Kim, YB, Park, TG *et al.* (2011). Antifibrotic effect of MMP13-encoding plasmid DNA delivered using polyethylenimine shielded with hyaluronic acid. *Mol Ther* **19**: 355–361.
12. Abe, H, Kamimura, K, Kobayashi, Y, Ohtsuka, M, Miura, H, Ohashi, R *et al.* (2016). Effective prevention of liver fibrosis by liver-targeted hydrodynamic gene delivery of matrix metalloproteinase-13 in a rat liver fibrosis model. *Mol Ther Nucleic Acids* **5**: e276.
13. Kamimura, K and Liu, D (2008). Physical approaches for nucleic acid delivery to liver. *AAPS J* **10**: 589–595.
14. Liu, F, Song, Y and Liu, D (1999). Hydrodynamics-based transfection in animals by systemic administration of plasmid DNA. *Gene Ther* **6**: 1258–1266.
15. Yokoo, T, Kamimura, K, Suda, T, Kanefuji, T, Oda, M, Zhang, G *et al.* (2013). Novel electric power-driven hydrodynamic injection system for gene delivery: safety and efficacy of human factor IX delivery in rats. *Gene Ther* **20**: 816–823.
16. Yoshino, H, Hashizume, K and Kobayashi, E (2006). Naked plasmid DNA transfer to the porcine liver using rapid injection with large volume. *Gene Ther* **13**: 1696–1702.
17. Aliño, SF, Herrero, MJ, Noguera, I, Dasí, F and Sánchez, M (2007). Pig liver gene therapy by noninvasive interventionist catheterism. *Gene Ther* **14**: 334–343.
18. Eastman, SJ, Baskin, KM, Hodges, BL, Chu, Q, Gates, A, Dreusicke, R *et al.* (2002). Development of catheter-based procedures for transducing the isolated rabbit liver with plasmid DNA. *Hum Gene Ther* **13**: 2065–2077.
19. Fabre, JW, Grehan, A, Whitehorne, M, Sawyer, GJ, Dong, X, Salehi, S *et al.* (2008). Hydrodynamic gene delivery to the pig liver via an isolated segment of the inferior vena cava. *Gene Ther* **15**: 452–462.
20. Khorsandi, SE, Bachellier, P, Weber, JC, Greget, M, Jaeck, D, Zacharoulis, D *et al.* (2008). Minimally invasive and selective hydrodynamic gene therapy of liver segments in the pig and human. *Cancer Gene Ther* **15**: 225–230.
21. Carreño, O, Sendra, L, Montalvá, E, Miguel, A, Orbis, F, Herrero, MJ *et al.* (2013). A surgical model for isolating the pig liver *in vivo* for gene therapy. *Eur Surg Res* **51**: 47–57.
22. Kamimura, K, Suda, T, Xu, W, Zhang, G and Liu, D (2009). Image-guided, lobe-specific hydrodynamic gene delivery to swine liver. *Mol Ther* **17**: 491–499.
23. Kamimura, K, Suda, T, Zhang, G, Aoyagi, Y and Liu, D (2013). Parameters affecting image-guided, hydrodynamic gene delivery to swine liver. *Mol Ther Nucleic Acids* **2**: e128.
24. Kamimura, K, Kanefuji, T, Yokoo, T, Abe, H, Suda, T, Kobayashi, Y *et al.* (2014). Safety assessment of liver-targeted hydrodynamic gene delivery in dogs. *PLoS One* **9**: e107203.
25. Yeikilis, R, Gal, S, Kopeiko, N, Paizi, M, Pines, M, Braet, F *et al.* (2006). Hydrodynamics based transfection in normal and fibrotic rats. *World J Gastroenterol* **12**: 6149–6155.
26. Granzow, M, Schierwagen, R, Klein, S, Kowallick, B, Huss, S, Linhart, M *et al.* (2014). Angiotensin-II type 1 receptor-mediated Janus kinase 2 activation induces liver fibrosis. *Hepatol* **60**: 334–348.
27. Yang, L, Kwon, J, Popov, Y, Gajdos, GB, Ordog, T, Brekken, RA *et al.* (2014). Vascular endothelial growth factor promotes fibrosis resolution and repair in mice. *Gastroenterol* **146**: 1339–50.e1.
28. Chen, SW, Zhang, XR, Wang, CZ, Chen, WZ, Xie, WF and Chen, YX (2008). RNA interference targeting the platelet-derived growth factor receptor beta subunit ameliorates experimental hepatic fibrosis in rats. *Liver Int* **28**: 1446–1457.
29. Du, SL, Pan, H, Lu, WY, Wang, J, Wu, J and Wang, JY (2007). Cyclic Arg-Gly-Asp peptide-labeled liposomes for targeting drug therapy of hepatic fibrosis in rats. *J Pharmacol Exp Ther* **322**: 560–568.
30. Zhang, G, Budker, V and Wolff, JA (1999). High levels of foreign gene expression in hepatocytes after tail vein injections of naked plasmid DNA. *Hum Gene Ther* **10**: 1735–1737.
31. Suda, T, Gao, X, Stolz, DB and Liu, D (2007). Structural impact of hydrodynamic injection on mouse liver. *Gene Ther* **14**: 129–137.
32. Zhang, G, Gao, X, Song, YK, Vollmer, R, Stolz, DB, Gasiorowski, JZ *et al.* (2004). Hydroporation as the mechanism of hydrodynamic delivery. *Gene Ther* **11**: 675–682.
33. Suda, T and Liu, D (2007). Hydrodynamic gene delivery: its principles and applications. *Mol Ther* **15**: 2063–2069.
34. Kamimura K, Suda T, Liu D. (2015) Hydrodynamic gene delivery. In: Olivia M, Mansoor MA (eds). *Advances and Challenges in the Delivery of Nucleic Acid Therapies*, Future Science: London, pp 43–56.
35. Kamimura K, Suda T, Kanefuji T, Yokoo T, Abe H, Kobayashi Y, *et al.* (2016) Image-guided hydrodynamic gene delivery to the liver: Toward clinical applications. In: Terai S, Suda T (eds). *Gene Therapy and Cell Therapy Through the Liver*, Springer Japan: Tokyo, pp 85–92.
36. Kamimura, K, Yokoo, T, Abe, H, Kobayashi, Y, Ogawa, K, Shinagawa, Y *et al.* (2015). Image-guided hydrodynamic gene delivery: current status and future directions. *Pharmaceutics* **7**: 213–223.
37. Kamimura, K, Zhang, G and Liu, D (2010). Image-guided, intravascular hydrodynamic gene delivery to skeletal muscle in pigs. *Mol Ther* **18**: 93–100.
38. Kamimura K, Abe H, Suda T, Aoyagi Y, Liu D (2013) Liver-directed gene therapy. *JSM Gastroenterol Hepatol* **1**: 1005.
39. Ueki, T, Kaneda, Y, Tsutsui, H, Nakanishi, K, Sawa, Y, Morishita, R *et al.* (1999). Hepatocyte growth factor gene therapy of liver cirrhosis in rats. *Nat Med* **5**: 226–230.
40. Khokha, R, Murthy, A and Weiss, A (2013). Metalloproteinases and their natural inhibitors in inflammation and immunity. *Nat Rev Immunol* **13**: 649–665.
41. Tag CG, Sauer-Lehnen S, Weiskirchen S, Borkham-Kamphorst E, Tolba RH, Tacke F, *et al.* (2015) Bile duct ligation in mice: induction of inflammatory liver injury and fibrosis by obstructive cholestasis. *J Vis Exp* **96**: 52438.
42. Suda, T, Suda, K and Liu, D (2008). Computer-assisted hydrodynamic gene delivery. *Mol Ther* **16**: 1098–1104.
43. Higashiyama, R, Inagaki, Y, Hong, YY, Kushida, M, Nakao, S, Niioka, M *et al.* (2007). Bone marrow-derived cells express matrix metalloproteinases and contribute to regression of liver fibrosis in mice. *Hepatol* **45**: 213–222.
44. Sakaida, I, Terai, S, Yamamoto, N, Aoyama, K, Ishikawa, T, Nishina, H *et al.* (2004). Transplantation of bone marrow cells reduces CCl4-induced liver fibrosis in mice. *Hepatol* **40**: 1304–1311.
45. Terai, S, Tanimoto, H, Maeda, M, Zaitsu, J, Hisanaga, T, Iwamoto, T *et al.* (2012). Timeline for development of autologous bone marrow infusion (ABMi) therapy and perspective for future stem cell therapy. *J Gastroenterol* **47**: 491–497.
46. Vrekoussis, T, Chaniotis, V, Navrozoglou, I, Dousias, V, Pavlakis, K, Stathopoulos, EN *et al.* (2009). Image analysis of breast cancer immunohistochemistry-stained sections using ImageJ: an RGB-based model. *Anticancer Res* **29**: 4995–4998.

Supplementary Information accompanies this paper on the Molecular Therapy–Nucleic Acids website (http://www.nature.com/mtna)